Oxidation Enthalpies for Reduction of Ceria Surfaces

Gong Zhou[1], Parag R. Shah[1], Tiziano Montini[2], Paolo Fornasiero[2], and Raymond J. Gorte[1*]

[1]Department of Chemical and Biomolecular Engineering
University of Pennsylvania
Philadelphia, PA 19104, USA

[2]Department of Chemistry, CENMAT and INSTM
University of Trieste, via L. Giorgieri 1, 34127 Trieste, Italy

Abstract

The thermodynamic properties of surface ceria were investigated through equilibrium isotherms determined by flow-titration and coulometric-titration measurements on high-surface-area ceria and ceria supported on La-modified alumina (LA). While the surface area of pure ceria was found to be unstable under redox conditions, the extent of reduction at 873 K and a $P(O_2)$ of $1.6x10^{-26}$ atm increased with surface area. Because ceria/LA samples were stable, equilibrium isotherms were determined between 873 and 973 K on a 30-wt% ceria sample. Oxidation enthalpies on ceria/LA were found to vary with the extent of reduction, ranging from -500 kJ/mol O_2 at low extents of reduction to near the bulk value of -760 kJ/mol O_2 at higher extents. To determine whether +3 dopants could affect the oxidation enthalpies for ceria, isotherms were measured for Sm^{+3}-doped ceria (SDC) and Y^{+3}-doped ceria. These dopants were found to remove the phase transition observed in pure ceria below 973 K but appeared to have minimal effect on the oxidation enthalpies. Implications of these results for catalytic applications of ceria are discussed.

Key Words: Ceria, Coulometric titration, thermodynamic properties, surface reduction, oxidation enthalpy.

Introduction

Ceria-based materials have been used for many years in automotive emissions control for Oxygen-Storage Capacitance (OSC) [1-3] and are finding many new applications as supports for water-gas-shift catalysts [4-12], supports for reforming catalysts [13,14], and as hydrocarbon oxidation catalysts in diesel emissions [15,16]. In all of these applications, it is likely that the ability of cerium to cycle between Ce^{+3} and Ce^{+4} is crucial. Since the reducibility of ceria is strongly affected by the presence of dopants and the structure of the material, much of the catalyst literature has focused on developing ways to tailor the properties of ceria. It is therefore surprising that our fundamental understanding of how structure and composition affect ceria reducibility is really rather poor. For example, only recently has it been shown that the thermodynamic properties, not simply the reduction kinetics, of ceria-zirconia solid solutions differ dramatically from those of pure ceria [17,18].

Even with pure ceria, there is evidence that the redox properties of nano-crystallites used in catalysis are very different from the thermodynamic properties of the ceria that was used for the data tabulated in the handbooks. The tabulated thermodynamic properties were all measured on materials that had been calcined at high temperatures, mostly for application in steel manufacturing [19], so that the tabulated values may not apply to catalytic materials. First, it has been shown that high-temperature calcination of ceria can cause severe deactivation of the catalytic properties, beyond what can be explained by surface-area effects [20-23]. Second, with nano-crystalline ceria, there is a report that desorption of O_2 can be observed into a flowing carrier gas at temperatures as low as 623 K [24]. This would suggest a reduction enthalpy that is only ~30% of the tabulated value based on typical relationships between heats of adsorption and desorption activation energies. Even in the absence of re-adsorption, a desorption peak temperature of 623 K would correspond to an activation energy for desorption of roughly 200 kJ/mol of O_2, compared to the tabulated value for the oxidation enthalpy for Ce_2O_3 of -760 kJ/mol-O_2 [25]. Third, electrical conductivity measurements have indicated that the enthalpy of reduction for ceria nano-particles is half that of bulk ceria [26,27]. Finally, Rodriguez and coworkers used X-ray Near Edge Spectroscopy and other techniques to suggest that ceria and ceria-zirconia nano-particles reduce more easily [28].

The question arises as to why the thermodynamics of reduction should be different for nano-particles or other low-temperature forms of ceria. One possibility is structural. For

example, the reduced species could remain in a cubic $CeO_{(2-x)}$ form rather than going to the hexagonal Ce_2O_3; at least some of the energy of reduction of bulk ceria is associated with structural changes. That crystallite size can affect structure is known with zirconia. Nano-particles of zirconia exhibit a tetragonal structure at room temperature and do not revert to their thermodynamically stable, monoclinic structure until larger particles are formed [29]. However, even large ceria crystallites do not convert to the hexagonal form for low extents of reduction and the enthalpy of forming O_2 from $CeO_{(2-x)}$ has been reported to be essentially independent of x, even down to quite low values of x [30,31].

Another possibility is that surface effects could play a role. Indeed, the work by Kim, et al, mentioned earlier [24], correlated oxygen uptake and release with the surface area of nano-particles. Another experimental study pointing towards the importance of surface reduction found that nano-rods synthesized to preferentially expose CeO_2(111) planes are easier to reduce than normal nano-particles [32]. That certain surfaces of ceria are more easily reduced has also been argued in theoretical studies. For example, a recent calculation has argued that (100) surfaces are preferentially reduced [33]. It is worth noting that complete reduction of a (100) surface gives ~5.7 μmol of oxygen/m^2 (This is simply 25% of the oxygen at the surface.), so that surface reduction of a 10-nm particle (~85 m^2/g) would correspond to ~17% of the bulk reduction.

Still another explanation for why nano-particles might be easier to reduce is that "low-temperature" ceria is likely to contain many defects. This picture has been offered by Egami and coworkers [34], who have argued that some oxygen ions are located in interstitial sites, rather than in the normal fluorite lattice sites, when ceria has never been calcined above 973 K. They proposed that interstitial oxygen is much easier to remove than normal oxygen, although they appear to have been considering primarily the kinetics of reduction, not the energetics. Certainly, it would be important to know if interstitial oxygen is bound so much more loosely than normal lattice oxygen.

In the present study, we set out to measure the thermodynamics of ceria oxidation and reduction in materials more closely related to those used in catalysis. The methods we have used are similar to those employed in the thermodynamic measurements of ceria-zirconia solid solutions, where equilibrium isotherms for $P(O_2)$ were measured as a function of temperature using flow titration or Coulometric titration [18]. Both methods involve measuring the oxygen

stoichiometry of ceria (e.g., x in $CeO_{(2-x)}$) in the presence of fixed partial pressures of H_2 and H_2O. Equilibrium for H_2 oxidation, $H_2 + ½O_2 = H_2O$, then establishes an O_2 fugacity according to Equation 1).

$$P(O_2)^{½} = K_{equilib}^{-1} * P(H_2O)/P(H_2) \quad 1)$$

Since the equilibrium constant for oxidation of $CeO_{(2-x)}$ is equal to $P(O_2)^{-½}$, the Gibbs Free Energy, ΔG, can be determined as a function of x. Finally, oxidation enthalpies, ΔH, can be determined from the temperature dependence of the equilibrium isotherms using Equation 2).

$$\Delta H = -R\, \delta \ln(P(O_2))/\delta(1/T)\big|_x \quad 2)$$

Because the surface area of pure ceria is not stable under redox cycling, the measurements with high-surface-area ceria were performed with samples supported on γ-Al_2O_3. To minimize formation of ceria aluminates [35] and maintain surface area following high-temperature treatment, the alumina was doped with 11.5-wt% La_2O_3. The effect of rare-earth dopants was also studied on bulk samples doped with Y^{+3} and Sm^{+3}.

Experimental Section

Samples

In order to prepare high-surface-area samples with optimal stability, the ceria was prepared by precipitation of cerium hydroxide in ammonium hydroxide solutions, followed by consecutive hydrothermal and alcothermal treatment. $Ce(NO_3)_3 \bullet 6H_2O$ (Aldrich 99.99 %) was dissolved in distilled water, after which the solution was added drop wise to a 10% NH_4OH solution under vigorous stirring. H_2O_2 (35%) was then added to the suspension and the mixture was stirred for 40 min before filtering. The precipitate was placed in an autoclave with water and heated slowly to 363 K, at which point the pressure inside the autoclave was 10 bar. The sample was left under those conditions for 12 h. After lowering the temperature and decreasing the pressure, the sample was placed in a round flask with iso-propanol (Carlo Erba 99.7 %) and boiled under total reflux conditions for 5 h. After cooling, the precipitate was filtered, washed with iso-propanol, and dried at 393 K for 12 h. The use of an autoclave and refluxing/washing in iso-propanol was to increase surface area and to enhance pore stability. The treatments favour crystallization and hydroxide-to-oxide transformation as well as prevent pore collapsing during drying. Finally, the sample was calcined in air at a heating rate of 1.5 K/min from room temperature to 873 K, where it was held for 5 h.

Surface areas were determined by the BET method using N_2 as the adsorbent. X-ray diffraction (XRD) data was collected using a Rigaku Geigerflex diffractometer with CuKα radiation (λ = 1.5405 Å). The average crystallite sizes of the oxidized samples were determined using the width of (220) diffraction peak and the Debye-Scherrer equation [38].

The specific surface area of ceria prepared in the above manner was 89 m^2/g. Samples with surface areas of 35 m^2/g and 25 m^2/g were prepared by reducing the initial sample in dry H_2, then oxidizing it in air, at either 873 or 973 K, respectively. A 3-m^2/g sample was obtained by calcining ceria at a temperature of 1323 K.

For the supported-ceria samples, we first prepared La-modified alumina (LA, 11.5-wt% La_2O_3 on γ-Al_2O_3, Alfa Aesar) by impregnating the alumina with an aqueous solution of $La(NO_3)_3$•$6H_2O$ (Alfa Aesar). After impregnation, the supports were dried in air at 373 K for 4 h to remove excess water and then calcined at 973 K in air for 5 h [36,37]. Ceria was added to the LA support by impregnation with aqueous solutions of $Ce(NO_3)_3$•$6H_2O$. After impregnation, the samples were again dried in air at 373 K for 4 h to remove excess water and then calcined at 973 K in air for 5 h to form a stable catalyst.

Fig. 1 shows XRD data for ceria supported on LA as a function of ceria loading, after the samples had been stabilized by at least one redox cycle at 973 K. (The 15- and 50-wt% ceria samples had gone through one redox cycle and the 30-wt% sample had gone through six redox cycles.) In our LA samples, the La_2O_3 loading corresponds to approximately one monolayer of $LaAlO_3$ and was added to prevent formation of ceria aluminates, $CeAlO_3$, which prevents Ce^{3+}/Ce^{4+} cycling. The XRD pattern of the LA support in Fig 1a is typical of γ-Al_2O_3. It is likely that the $LaAlO_3$ phase is not observed in the diffraction pattern because of the relatively low loading. The important point is that there is no evidence for formation of $CeAlO_3$ in the ceria-containing samples, even after redox cycling. Figs. 1b through 1d indicate that ceria in each of the samples exists in the bulk-ceria, fluorite structure. The lattice constant for the ceria phase was calculated to be 0.541 nm using the location of the (220) diffraction peak, consistent with pure ceria. As expected, the crystallite sizes calculated from the XRD line widths were found to increase with ceria loading, as reported in Table 1.

Solid solutions of ceria with Y_2O_3 and Sm_2O_3, $Ce_{0.8}Y_{0.2}O_{1.9}$, and $Ce_{0.8}Sm_{0.2}O_{1.9}$, were prepared using citric acid, as previously described [38,39]. Stoichiometric amounts of $Ce(NO_3)_3$•$6H_2O$ and either $Y(NO_3)_3$•$6H_2O$ or $Sm(NO_3)_3$•$6H_2O$ were dissolved in distilled water

and mixed with aqueous citric acid (≥99.5%, Aldrich) to produce a solution with a citric-acid:metal-ion ratio of 1:2. The solutions were stirred vigorously at room temperature for one hour and then the water was removed by evaporation. Finally, the resulting solids were heated in air at 723 K for 5 h to produce the mixed oxides. Analysis of the lattice parameters in previous work showed that this preparation procedure results in the formation of solid solutions for compositions used in the present study [39].

Equilibrium Measurements

Two techniques were used to measure the equilibrium oxidation isotherms, both of which have been described in detail elsewhere [17,18]. The first, flow titration, involved placing between 0.5 and 1.0 g of sample in a quartz-tube flow reactor, then exposing the reduced sample to a flowing mixture of H_2 and H_2O at the temperature of interest for 3 h. The water vapor was introduced into the gas stream by passing pure H_2 through a temperature-controlled, water bubbler and the H_2O partial pressure was evaluated from the equilibrium vapor pressure. After equilibration of the sample in the H_2-H_2O mixture, the reactor was purged with dry He for 0.5 h. Finally, the oxidation state of the sample was determined by measuring the amount of oxygen required for complete re-oxidation. This was accomplished by flowing air (21% O_2 and 79% N_2) over the sample at a rate of 4.3 ml/min and measuring the composition of the effluent gas from the reactor using a quadrupole mass spectrometer. The N_2 signal from the air was used as an internal standard for determining the amount of O_2 consumed.

It was possible to show that equilibrium was achieved in the sample by the fact that the extent of reduction at a particular H_2-H_2O ratio was independent of whether we started with an oxidized or a reduced sample. However, equilibrium was reached more quickly starting with samples that had been reduced in dry H_2 prior to exposing them to H_2-H_2O mixtures. We also observed that equilibrium was achieved more quickly when the samples were doped with precious metals. Therefore,most measurements in the present study were performed on samples having 1 wt% Pd, added using an aqueous solution of $(NH_3)_4Pd(NO_3)_2$ (99.9%, Alfa Aesar), followed by sample calcination at 723 K in air for 5 h.

Because the H_2:H_2O ratio can only be controlled over a limited range in a flow system, coulometric titration was used to obtain equilibrium information at higher $P(O_2)$. In this technique, the $P(O_2)$ of the gases over an equilibrated sample are measured electrochemically with an oxygen sensor [18]. In our apparatus, the sample was placed in a sealed container at the

temperature of interest and reduced by passing a mixture of He, H_2, and H_2O over it. Then the sample was sealed in the gas mixture (for the present study, ~90% He, 10% H_2, and 0.3% H_2O) and the equilibrium $P(O_2)$ was measured with an oxygen sensor. The oxygen sensor was essentially a solid oxide fuel cell that was part of the container wall and could also be used to add or remove oxygen from the system through application of a potential across the ion-conducting, YSZ membrane. Because 1 C is equivalent to 2.6 μmol O_2, electrochemical addition of oxygen is very precise. Since 10^{-20} atm corresponds to less than one molecule in the coulometric-titration apparatus, it should be recognized that the $P(O_2)$ is a fugacity established by equilibrium between H_2 and H_2O over much of the $P(O_2)$ range that was investigated.

In a previous coulometric-titration study which used Pt as the sample-side electrode of the oxygen sensor, measurements could not be performed at $P(O_2)$ corresponding to a sensor potential greater than approximately 0.85 V because of the tendency of Pt electrodes to react with ZrO_2 to form $PtZr_3$ under highly reducing conditions [40]. Formation of the alloy provides a thermodynamic driving force for removal of oxygen from zirconia and this loss of oxygen cannot be distinguished from reduction of the sample. To avoid this problem in the present study, we replaced the Pt electrode with Ag. Tests of the coulometric-titration apparatus without a sample showed that there was no reduction of zirconia at potentials as high as at least 1.1 V, a potential that corresponds to a $P(O_2)$ of approximately 10^{-24} atm at 973 K. However, because there was a significant amount of gas-phase H_2 over the sample at these potentials, it was necessary in the initial pulses to calculate the fraction of added oxygen that was used to convert H_2 to H_2O.

The criterion we used for establishing equilibrium in coulometric titration was that the potential of the oxygen sensor changed by less than 1 mV/h. The time required for achieving equilibrium depends on the temperature and the sample but was typically two days after the addition of oxygen to the sample below 873 K in the present experiment. Equilibrium was reached much faster, usually in 4 to 5 h, when the sample temperature was changed without the addition of oxygen. Furthermore, while it was difficult to establish reversibility by electrochemically pumping oxygen from the sample (the pumping rates out of the cell were simply too low), reversibility with temperature changes was checked and achieved in all cases.

Results

High-Surface-Area Ceria and Ceria/LA

Initial attempts to measure the equilibrium properties of high-surface-area ceria using flow titration were unsuccessful because the surface areas of the sample were not stable under redox cycling at 873 K, even with an initial sample calcination temperature of 873 K. The extent of sample reduction in a specific H_2-H_2O mixture decreased with each reduction-oxidation cycle. Together with the change in sample reducibility, we observed a dramatic decrease in the ceria surface area, from an initial value of 89 m^2/g to 35 m^2/g after a single redox cycle at 873 K.

To demonstrate the correlation between reducibility and surface area, Table 2 shows the equilibrium stoichiometries of samples exposed to a 10% H_2O-90% H_2 mixture at 873 K as a function of the ceria surface area, measured prior to reduction. The calculated $P(O_2)$, assuming equilibrium for H_2 oxidation, is $1.6x10^{-26}$ atm under these conditions. In agreement with published data for bulk ceria [17,30-31], 3-m^2/g ceria remains almost completely oxidized at this $P(O_2)$, with an O:Ce ratio of 1.98. The extent of reduction in the samples increased regularly with the surface areas, with the 89-m^2/g sample showing an O:Ce ratio of 1.92 at the same $P(O_2)$. Based on the amount of oxygen that would be removed by surface reduction of $CeO_2(100)$, 17.5% of the removable oxygen in the 89-m^2/g sample should be considered surface oxygen. Because complete removal of only the surface oxygen from the 89-m^2/g ceria would lead to a O:Ce ratio of 1.918, a value close to that measured experimentally, it is reasonable to explain the results in Table 2 by assuming there is a different equilibrium isotherm for the surface and bulk ceria, with surface ceria being primarily reduced and the bulk primarily oxidized at the conditions of this experiment.

In order to study the effect of surface ceria more carefully, we prepared samples of ceria on La-modified alumina (LA), with ceria loadings of 15, 30, and 50 wt%. The LA support was chosen because of its high surface area and excellent thermal stability under redox conditions. Also, we anticipated that interactions between ceria and LA would have a negligible effect on the reducibility of ceria, in contrast to the strong promotion of ceria reduction observed with ceria on zirconia [35,41]. Unlike pure ceria, the ceria/LA samples were found to be quite stable to redox cycling. For example, the 30%-ceria sample showed negligible change in the extent of reduction in fixed H_2O:H_2 compositions after six cycles at 973 K.

As an initial test of the relative reducibility of the ceria/LA samples, we measured the O:Ce ratio for the three samples after exposing them to 10% H_2O-90% H_2 mixtures at 973 K ($P(O_2) = 1.8 x10^{-23}$ atm), with the results shown in Table 1. These experiments were performed

at a higher temperature than those on the pure ceria because equilibrium was achieved more rapidly at 973 K and the ceria/LA samples were found to be unaffected by the higher temperatures. The LA support without ceria underwent a small reduction, 80 μmol O/g, which was subtracted from the amount of oxygen required to oxidize ceria in the other samples. (No Pd was added to the LA support in this experiment, so that reduction must be of the LA support itself.) While the O:Ce ratio for pure, 3-m^2/g ceria was again 1.98 under these new conditions, the ceria/LA samples were reduced much more substantially. The ceria in the 15-wt% sample was reduced almost completely to Ce_2O_3 (O:Ce = 1.63) while even the 50-wt% ceria sample had an O:Ce ratio of 1.87. We attempted to correlate the higher reducibility of the ceria/LA samples with the surface areas of the ceria, calculating the ceria area assuming spherical ceria particles with a diameter equal to the crystallite size measured in XRD. However, based on these calculations, the fraction of surface ceria on the 50-wt% ceria/LA sample, 16%, was actually lower than the fraction of surface ceria on the 89-m^2/g sample. We suggest that the calculations based on XRD crystallite size do not accurately reflect the true surface ceria but we cannot rule out the possibility that there are strong interactions between ceria and LA that could affect ceria reducibility.

A more complete set of isotherms at 873, 923, and 973 K are shown in Fig. 2 for the 30-wt% ceria/LA sample, together with the corresponding isotherms for bulk ceria that were reported previously [17]. The data for bulk ceria was taken using flow-titration measurements, implying that the O:Ce stoichiometries have been determined directly. The data for the ceria/LA sample were taken using coulometric titration. While oxygen addition is very precise in coulometric titration, the absolute stoichiometry must be known at some temperature and $P(O_2)$ in order to determine the absolute stoichiometries. In the present experiment, the sample was assumed to be fully oxidized at a $P(O_2)$ of 10^{-2} atm. Using this reference, Fig. 2 shows that the O:Ce ratio at 973 K and a $P(O_2)$ of 1.8 x10^{-23} atm is 1.76, a value slightly lower than that given in Table 1. However, the data in Table 1 were corrected for reduction of the LA support; including this correct in Fig. 2 would cause the absolute O:Ce ratios for the two experiments to agree extremely well. Finally, the flow-titration data on this same sample, which is included in Fig. 2, shows excellent agreement with coulometric titration.

For bulk ceria, most oxidation occurs over a very narrow range of $P(O_2)$ in this temperature range because there are two ceria phases, a reduced phase and a more oxidized

phase, in equilibrium at 973 K and below [42]. For ceria oxidation at temperatures above 1073 K, there is only a single ceria phase with a varying oxygen stoichiometry. Therefore, the oxidation isotherms take on a slope at the higher temperatures due to the fact that oxygen is being added gradually over a range of $P(O_2)$. The isotherms on the ceria/LA sample exhibit a more gradual increase in O:Ce stoichiometry with $P(O_2)$, even more than bulk ceria at higher temperatures.

The oxidation enthalpy, $-\Delta H$, can be calculated from the temperature dependence of the isotherms, using Equation 2; and we have plotted these values as a function of O:Ce ratio in Fig. 3. For pure ceria, the enthalpies are between 750 and 800 kJ/mol-O_2 for O:Ce ratios between 1.90 and 1.95. This is in excellent agreement with the handbook value of 760 kJ/mol-O_2 [25]. Furthermore, based on the literature [31], the oxidation enthalpies for ceria are constant for O:Ce ratios between 1.85 and 2.0. By contrast, the oxidation enthalpies for ceria/LA are a strong function of oxygen stoichiometry in the ceria, starting above 700 kJ/mol-O_2 for deep ceria reduction and decreasing to 500 kJ/mol-O_2 as the sample becomes oxidized. The values shown here are consistent. Even for a well-dispersed ceria phase, deep reduction must involve bulk ceria, so that the oxidation enthalpies would be expected to approach 760 kJ/mol-O_2 at the lowest O:Ce ratios. Likewise, the oxygen added at higher $P(O_2)$ is much less tightly bound.

Interestingly, the most weakly bound oxygen on the ceria/LA sample is associated with $-\Delta H$ of 500 kJ/mol-O_2, a value very close to the oxidation enthalpy of ceria-zirconia solid solutions, 520 kJ/mol-O_2 [19]. It may be fortuitous but one of our laboratories found that ceria-zirconia solid solutions showed essentially identical activity to that of pure ceria for oxidation of n-butane [39]. Unlike the ceria/LA sample, the oxidation enthalpies on the ceria-zirconia solid solutions were found to be independent of the extent of sample reduction; however, steady-state reactions likely involve only the surface oxygen.

Rare-Earth Doped Ceria

Because it was necessary to add lanthana at the surface of the alumina to prevent reaction on the ceria/LA samples, there is the question whether the enhanced reducibility of some samples might be due to doping of the ceria by La^{3+}. To investigate whether the enhanced reducibility of the ceria/LA samples could be due to La doping of ceria, we examined Sm^{+3}-doped ceria (SDC) and Y^{+3}-doped ceria (YDC). The reason for examining SDC and YDC solid solutions is that La^{+3}-doped ceria is reported to be unstable when heavily reduced [43].

Furthermore, Sm^{+3} is one of the best dopants for increasing ionic conductivity in ceria [44] and was observed to have a much larger effect on activity for n-butane oxidation [39], so that changes in the redox properties are expected to be much more significant. We considered Y^{+3} doping, which has less effect on the conductivity and catalytic activity than Sm^{+3}, to determine how general the results obtained with SDC are.

Fig. 4 shows oxygen isotherms for the SDC sample at 873, 923, 973, 1073, and 1173 K, measured using the flow-titration method. The isotherms are similar to those published for pure ceria [17], with one exception. The isotherms for SDC show no change in shape between 973 and 1073 K. As discussed earlier, the change in the slope of the isotherms for ceria between 973 and 1073 K is due to the presence of two phases for the partially reduced samples at the lower temperatures, whereas the oxygen vacancies are completely soluble in ceria at the higher temperatures. With SDC, the oxygen vacancies show complete solubility at all temperatures. Fig. 5 shows the change in isotherm shape for pure ceria, as well as the lack of a change in SDC, by comparing data at 973 and 1073 K for these two materials. The figure also shows that the isotherms for SDC and YDC at 973 K are essentially identical.

However, the most important point to note is that the oxidation enthalpies are not strongly affected by Sm^{+3} doping, as shown in Fig. 3. The enthalpies in the figure were calculated using Equation 2 and the data in Fig. 4. The enthalpies for SDC fall between -700 and -730 kJ/mol-O_2, in reasonable agreement with data for SDC in the published literature [30,31]. With pure ceria, oxidation enthalpies calculated from either high-temperature (1073 K and above) or low-temperature (973 K and below) data are the same, showing that the change in phase behavior does not affect oxygen binding energies. Apparently, rare-earth dopants also have minimal effect on the binding energies.

Discussion

The results described in this paper clearly demonstrate that the thermodynamic properties associated with high-surface-area ceria samples are different from that of bulk ceria. Assuming that the results for the LA-supported ceria are indicative of the surface ceria, oxygen binding energies at the surface are lower than those associated with the bulk by more than 200 kJ/mol O_2. On the other hand, the addition of +3 dopants into ceria does not appear to influence the redox properties of ceria substantially.

While it is tempting to associate surface oxygen with high catalytic activity, it is important to remember that, at least for some reactions, the activity of the ceria does not scale with surface area [20-23]. In particular, high-temperature treatment of ceria films has been shown to change the ability of the ceria surfaces to transfer oxygen [20-22]. It is likely that high temperatures change the structure of the surface in such a way that the oxygen is more strongly bound and that factors other than "surface versus bulk" are involved in the catalytic properties of ceria. For example, the surface of active ceria may be hydroxylated or consist of sites with special crystallographic geometries. How this would affect the oxygen binding is uncertain.

It is also possible that factors other than oxygen binding energy are important for understanding the catalytic properties of ceria. Indeed, factors other than binding energy must be important. There are other oxides with multiple oxidation states and similar oxidation enthalpies that are not as active as ceria for oxidation of hydrocarbons. Again, the site geometry will almost certainly affect how exposed the cations are to possible reactants. Identifying the structural factors that influence the catalytic properties of oxides is difficult, especially since the surfaces appear to evolve under reaction conditions.

That a ceria surface must undergo structural evolution under redox conditions is clear from the present study, since a sample, which had a surface area of 89 m^2/g after calcination at 873 K, had a surface area of only 35 m^2/g after a single redox cycle at the same temperature. Presumably, changes in the crystallographic orientations of the sites and the exposure of metal cations to the surface must occur along with the reduction in surface area.

It is also uncertain that the effect of having a support is simply to increase the fraction of ceria that is at the surface, and we cannot rule out the possibility that there are strong interactions between ceria and LA that could affect ceria reducibility. In the case for ceria supported on cubic zirconia [41], where there is strong evidence that zirconia influences ceria reducibility, that influence is observed for even very thick films [45]. Chemical interactions should not extend more than a few lattice parameters from the interface. For the effect of the interface to influence the ceria beyond a few layers, physical factors, such as induced strain or propagation of defect structures, must be important. Similar factors could influence the reducibility of ceria supported on La-modified alumina as well. Unfortunately, it was not possible for us to measure the thermodynamic properties on unsupported ceria.

While thermodynamic data clearly do not answer all questions about ceria catalysis, they do provide an important starting point for understanding reaction mechanisms on oxide catalysts. As shown by the previous results for ceria-zirconia solid solutions and the new data for high-surface-area ceria, data on bulk compounds that are reported in standard handbooks are not always applicable to catalytically interesting materials. Therefore, it is highly desirable to begin performing thermodynamic measurements on catalytically relevant materials. The present work is part of our attempt to begin obtaining this kind of information.

Conclusions:

The thermodynamic redox properties of ceria surfaces appear to differ significantly from that of bulk ceria. The magnitude of the oxidation enthalpies can be more than 200 kJ/mole O_2 lower at the surface, strongly affecting the ability of the material to release oxygen under reaction conditions. The results show that thermodynamic data for bulk compounds may not be relevant for catalytic applications and point out the need for obtaining thermodynamic information on catalytically relevant materials.

Acknowledgements:

This work was supported by the Department of Energy, Office of Basic Energy Sciences, Chemical Sciences, Geosciences and Biosciences Division, Grant DE-FG02-85ER13350.
P.F. and T.M. acknowledge FISR2002 “Nanosistemi inorganici ed ibridi per lo sviluppo e l'innovazione di celle a combustibile”.

References:

1) M. Sugiura, M. Ozawa, A. Suda, T. Suzuki, and T. Kanazawa, Bull. Chem. Soc. Jpn., 78 (2005) 752.
2) J. Kaspar, P. Fornasiero, N. Hickey, Catal. Today, 77 (2003) 419.
3) M. Shelef, G.W. Graham, R.W. McCabe, in: A. Trovarelli (Ed.), Catalysis by Ceria and Related Materials, Imperial College Press, London, 2002, p. 343.
4) A.F. Ghenciu, Current Opinion in Solid State and Materials Science 6 (2002) 389.
5) J.R. Ladebeck, J.P. Wagner, in: W. Vielstich, et al. (Eds.), Handbook of Fuel Cell Technology- Fundamentals, Technology, and Applications. Wiley, 2003 (Chapter17).
6) S. Y. Choung, M. Ferrandon, T. Krause, Catal. Today, 99 (2005) 257.
7) X. Liu, W. Ruettinger, X. Xu, and R. Farrauto, Appl. Catal. B, 56 (2005) 69.
8) Q. Fu, H. Saltsburg, M. Flytzani-Stephanopoulos, Science 301 (2003) 935.
9) S.L. Swartz, M.M. Seabaugh, C.T. Holt, W.J. Dawson, Fuel Cell Bull. 4 (2001) 7.
10) T. Bunluesin, R.J. Gorte, G.W. Graham, Appl. Catal. B 15 (1998) 107.
11) S. Hilaire, X. Wang, T. Luo, R.J. Gorte, J. Wagner, Appl. Catal. A 215 (2001) 271.
12) G. Jacobs, P. M. Patterson, U. M. Graham, D. E. Sparks, B. H. Davis, Appl. Catal. A, 269 (2004) 63.
13) R. Farrauto, S. Hwang, L. Shore, W. Ruettinger, J. Lampert, T. Giroux, Y. Liu, O., Ilinich, Annu. Rev. Mater. Res., 33 (2003) 1
14) R. Craciun, B. Shereck, and R.J. Gorte, Catalysis Letters, 51 (1998) 149
15) R. M. Heck and R. J. Farrauto, Appl. Catal. A, 221 (2001) 443.
16) A. Bueno-Lopez, K. Krishna, M. Makkee, J. A. Moulijn, J. Catal., 230 (2005) 237.
17) T. Kim, J. M. Vohs, and R. .J. Gorte, Industrial and Engineering Chemistry, 45 (2006) 5561-65.
18) P. R. Shah, T. Kim, G. Zhou, P. Fornasiero, and R. J. Gorte, Chemistry of Materials, 18 (2006) 5363-69
19) Cerium: A guide to its role in chemical technology, Molycorp, Inc., Mountain Pass, CA, (1992).
20) T. Bunluesin, R.J. Gorte, and G.W. Graham, Appl. Catal. B, 14 (1997) 105.
21) H. Cordatos, T. Bunluesin, J. Stubenrauch, J. M. Vohs, and R. J. Gorte, Journal of Physical Chemistry, 100 (1996) 785.
22) T. Bunluesin, R.J. Gorte, and G.W. Graham, Appl. Catal. B, 15 (1998) 107.
23) P. Fornasiero, J. Kapar and M. Graziani, J. Catal 167 (1997) 576.
24) S. Kim, R. Merkle, and J. Maier, Surf. Sci., 549 (2004) 196.
25) CRC Handbook, 84th Edition (2003-2004) p. 5-10.
26) Y.-M. Chiang, E. B. Lavik, and D. A. Blom, NanoStructured Materials, 9 (1997) 633.
27) Y.-M. Chiang, E. B. Lavik, I. Kosacki, H. L. Tuller, J. Y. Ying, Appl. Phys. Lett, 69 (1996) 187.
28) J. A. Rodriguez, J. C. Hanson, J.-Y. Kim, G. Liu, A. Iglesias-Juez, and M. Fernandez-Garcia, J. Phys. Chem. B, 107 (2003) 3535.
29) T. Chraska, A. H. King, and C. C. Berndt, Matls. Sci. & Eng. A286 (2000) 169.
30) M. Mogensen, N.M. Sammes, G.A. Tompsett, Solid State Ionics 129 (2000) 63.
31) M. Mogensen, "Catalysis by Ceria and Related Materials", A. Trovarelli, ed., Imperial College Press (2002) pp. 458, 459.
32) K. Zhou, X. Wang, X. Sun, Q. Peng, Y. Li, J. Catal., 229 (2005) 206.

33) T. X. T. Sayle, S. C. Parker, and D. C. Sayle, PCCP, 7 (2005) 2936.
34) E. Mamontov, T. Egami, R. Brezny, M. Koranne, S. Tyagi, J. Phys. Chem. B, 104 (2000) 11110.
35) O. Costa-Nunes, R.M. Ferrizz, R.J. Gorte, J.M. Vohs, Surface Science 592 (2005) 8.
36) M. Ozawa, J. of Alloys and Compounds, 408-412 (2006) 1090
37) M. Ozawa, H. Toda, S. Suzuki, Appl. Catal. B, 8 (1996) 141

38) J. Kaspar, P. Fornasiero, G. Baiducci, R. Di Monte, N. Hickey, V. Sergo, Inorganica Chimica Acta 349 (2003) 217.
39) S. Zhao and R. J. Gorte, Appl. Catal. A, 248 (2003) 9-18.
40) Werner, J.; Schmidfetzer, R. *Thermochim. Acta* (1988), *129*, 127-141.
41) O. Costa-Nunes, R. J. Gorte, and J. M. Vohs, Journal of Materials Chemistry, 15 (2005) 1520 - 1522.
42) D. J. M. Bevan and J. Kordis, J. Inorg. Nucl. Chem. 26 (1964) 1509.
43) H. J. Lang, K. Kunstler, G. Tomandl, Solid State ionics, 119 (1999) 127
44) K. Eguchi, T. Setoguchi, T. Inoue, and H. Arai, Solid State Ionics, 52 (1992) 165.
45) E.S. Putna, T. Bunluesin, X.L. Fan, R.J. Gorte, J.M. Vohs, R.E. Lakis, and T. Egami, Catal. Today, 50 (1999) 343.

Table 2

Measured O:Ce ratios for ceria as a function of surface area at a fixed $P(O_2)$. Each sample was equilibrated in a H_2-H_2O mixture (10% H_2O) [a] at 873 K.

SA (m^2/g)	3	25	35	89
O/Ce ratio	1.98	1.95	1.93	1.92
% surface[b]	0.6	4.9	6.9	17.5

[a] 10% H_2O in a H_2-H_2O mixture at 873 K corresponds to a $P(O_2)$ of 1.6×10^{-26} atm

[b] Based on the amount of oxygen that would be removed by surface reduction of $CeO_2(100)$, the data shows the percent of the removable oxygen in the sample that should be considered surface oxygen.

Table 1

Properties of the LA-supported ceria samples. For the O:Ce ratios, each sample was equilibrated in a H_2-H_2O mixture (10% H_2O) [a] at 973 K. The samples were initially calcined in air at 973 K for 6 h, then exposed to the H_2-H_2O mixture for an additional 6 h.

	LA	15wt%CeO_2/LA	30wt%CeO_2/LA [b]	50wt%CeO_2/LA
SA (m^2/g)	114	94	68	63
Crystallite size (Å)	-	68	75	101
O/Ce ratio[c]	-	1.63	1.77	1.86

[a] 10% H_2O in a H_2-H_2O mixture at 973 K corresponds to a $P(O_2)$ of 1.8×10^{-23} atm

[b] The 30-wt% CeO_2/LA sample was exposed to six oxidation-reduction cycles at 973 K, over a period of 100 h, prior to the measurements shown here.

[c] 80 μmol O/g was required for oxidation of the LA support after reduction; this value was subtracted from the ceria-containing samples in the calculation of the O/Ce ratio.

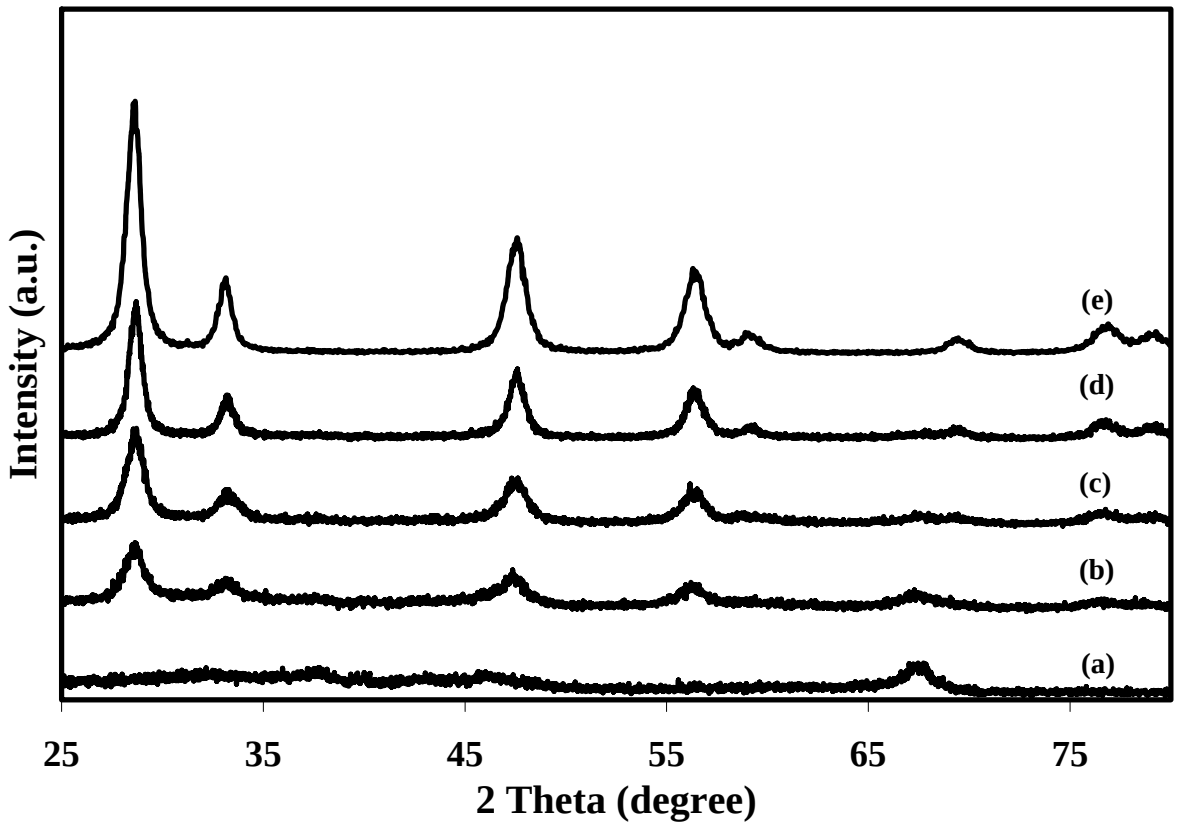

Figure 1. XRD patterns for ceria impregnated onto the LA support. Samples are shown following calcination at 973 K and the redox cycles discussed in the text. a) LA support, b) 15-wt% ceria/LA, c) 30-wt% ceria/LA, d) 50-wt% ceria/LA, and e) bulk ceria (3 m^2/g).

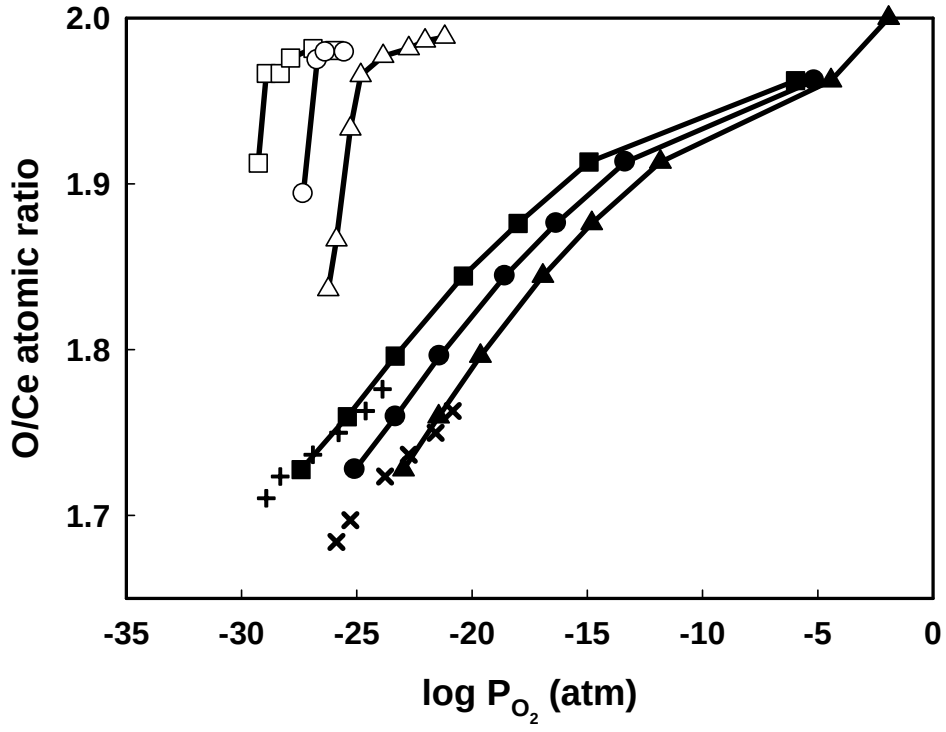

Figure 2. Oxidation isotherms for pure ceria (open symbols) and 30-wt% ceria/LA (filled symbols) at selected temperatures (■873K, ●923K, ▲973K). The results for pure ceria are taken from a previous publication [17] and were determined by flow titration, whereas the results for ceria/LA were obtained by coulometric titration. The (+) and (x) symbols show the isotherms for 30-wt% ceria/LA determined by flow titration at 873 and 973 K, respectively.

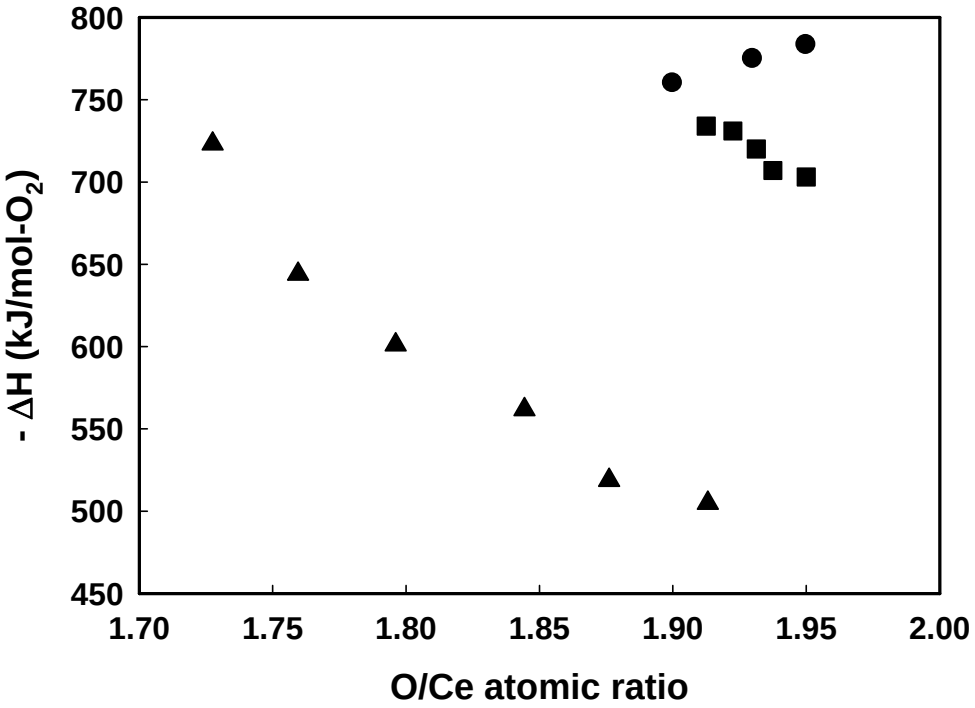

Figure 3. $-\Delta\hat{H}$ of oxidation at 973 K for (▲) 30-wt% ceria/LA, (■) $Ce_{0.8}Sm_{0.2}O_{1.9}$, and (●) pure ceria as a function of extent of reduction.

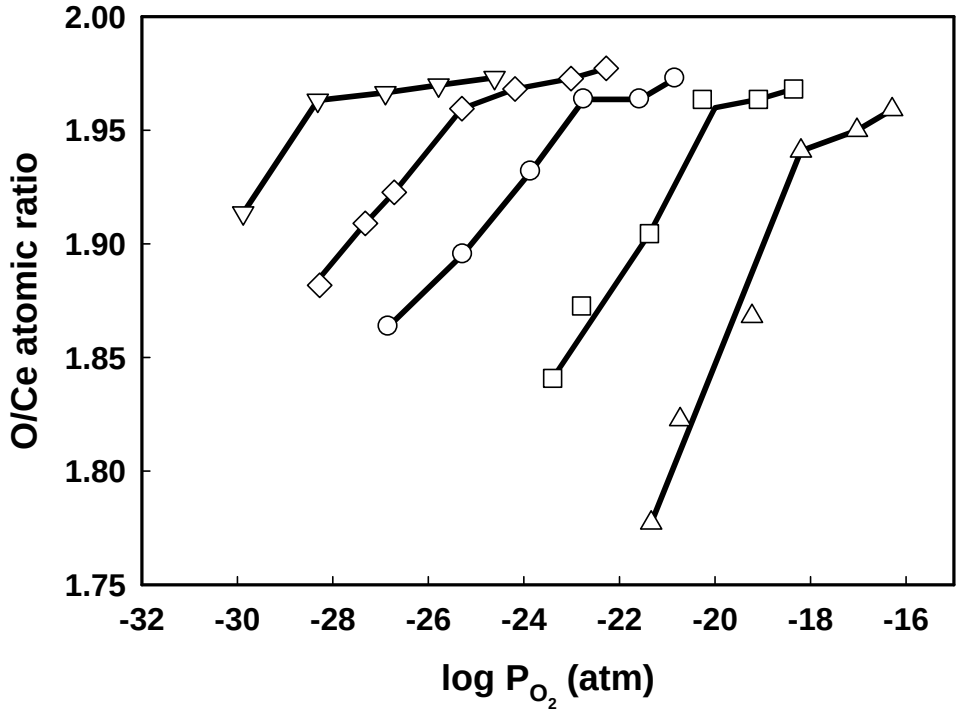

Figure 4). Oxidation isotherms for the $Ce_{0.8}$ $Sm_{0.2}O_{1.9}$ solid solution as a function of $P(O_2)$ temperature: ∇ 873 K, ◊ 923 K, ○ 973 K, □ 1073 K, and Δ 1173 K.

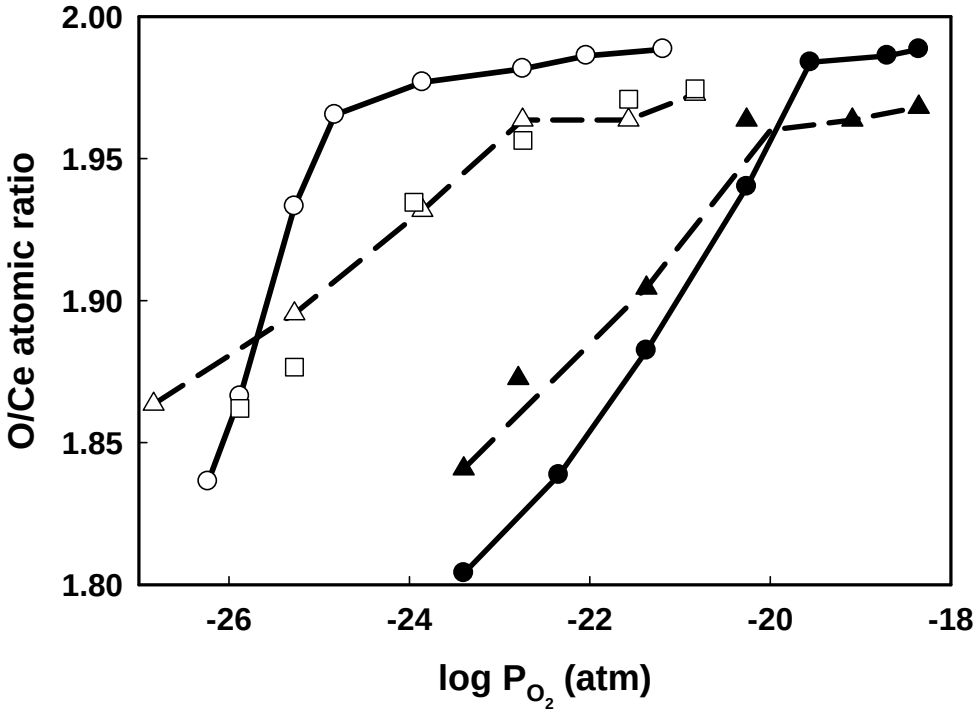

Figure 5. Oxidation isotherms for (○) pure CeO_2, (□) $Ce_{0.8}Y_{0.2}O_{1.9}$, and (Δ) $Ce_{0.8}Sm_{0.2}O_{1.9}$ solutions at 973 K. The filled symbols show isotherms for (●) pure CeO_2 and (▲) $Ce_{0.8}Sm_{0.2}O_{1.9}$ at 1073 K.